Formation of a Long-Lived Photoproduct with a Deprotonated Schiff Base in Proteorhodopsin, and Its Enhancement by Mutation of Asp227†

Eleonora S. Imasheva,‡ Kazumi Shimono,§ Sergei P. Balashov,*,‡ Jennifer M. Wang,‡ Uri Zadok,|| Mordechai Sheves,|| Naoki Kamo,§ and Janos K. Lanyi‡

Department of Physiology and Biophysics, University of California, Irvine, California 92697, Laboratory of Biophysical Chemistry, Graduate School of Pharmaceutical Sciences, Hokkaido University, Sapporo 060-0812, Japan, and Department of Organic Chemistry, The Weizmann Institute of Science, Rehovot, Israel

Received March 8, 2005; Revised Manuscript Received June 10, 2005

ABSTRACT: Proteorhodopsin, a retinal protein of marine proteobacteria similar to bacteriorhodopsin of the archaea, is a light-driven proton pump. Absorption of a light quantum initiates a reaction cycle (turnover time of ca. 50 ms), which includes photoisomerization of the retinal from the all-trans to the 13-cis form and transient deprotonation of the retinal Schiff base, followed by recovery of the initial state. We report here that in addition to this fast cyclic conversion, illumination at high pH results in accumulation of a long-lived photoproduct absorbing at 362 nm. This photoconversion is much more efficient in the D227N mutant in which the anionic Asp227, which together with Asp97 constitutes the Schiff base counterion, is replaced with a neutral residue. Upon illumination at pH 8.5, most of the D227N pigment is converted to the 362 nm species, with a quantum efficiency of ca. 0.2. The pK_a for this transition in the wild type is 9.6, but decreased to 7.5 after mutation of Asp227. The short wavelength of the absorption maximum of the photoproduct indicates that it has a deprotonated Schiff base. In the dark, this photoproduct is converted back to the initial pigment with a time constant of 30 min (in D227N, at pH 8.5), but it can be reconverted more rapidly by illumination with near-UV light. Experiments with "locked" retinal analogues which selectively exclude rotation around either the C9═C10, C11═C12, or C13═C14 bond show that formation of the 362 nm species involves isomerization around the C13═C14 bond. In agreement with this, retinal extraction indicates that the 362 nm photoproduct is 13-cis whereas the initial state is predominantly all-trans. A rapid shift of the pH from 8.5 to 4 greatly accelerates thermal reconversion of the 362 nm species to the initial pigment, suggesting that its recovery involving the thermal isomerization of the chromophore is controlled by ionizable residues, primarily the Schiff base and Asp97. The transformation to the long-lived 362 nm photoproduct is apparently a side reaction of the photocycle, a response to high pH, caused by alteration of the normal reprotonation and reisomerization pathway of the Schiff base.

Retinal proteins of the two major classes, photoreceptors and pumps, undergo photochemical reactions that are accompanied by large shifts of the chromophore absorption band. These shifts reflect mainly isomerization of the retinal and protonation changes of the Schiff base and its counterion. More subtle spectral transitions are caused by changes in protein conformation and chromophore environment. Spectroscopic studies of these light-induced absorption changes in combination with mutagenesis have provided valuable information about the mechanism of the functioning of visual rhodopsin, bacteriorhodopsin, and others (*2*−*6*). The cycle of photochemical conversions of bacteriorhodopsin constitutes the basis for light-induced proton transport by the purple membrane of halobacteria (*7*−*10*), whereas the photoreversible reactions of sensory rhodopsins I and II underline color discrimination and phototaxis (*3*, *11*). The photochromic properties of retinal pigments are interesting also as a potential source for applications in optical recording and information processing (*12*−*16*).

Recently, a new family of retinal proteins called proteorhodopsins has been discovered in uncultivated marine proteobacteria in the Pacific Ocean, Red Sea, Mediterranean Sea, and Sargasso Sea (*17*−*20*). This new family includes ∼800 variants (*20*). They fall in several groups, which differ in amino acid sequence, spectral properties (*21*, *22*), and important functional features such as the lifetime of the photocycle intermediates and the ability to generate photocurrents (*23*), implying the possible diversity of their functions.

The proteorhodopsin, produced from a gene found in proteobacteria of Monterey Bay [eBAC31A08 (*17*)] and expressed in *Escherichia coli*, exhibits a great deal of similarity to BR[1] (*17*, *24*), and like BR, it functions as a light-driven proton pump (*1*, *17*, *24*, *25*). However, PR exhibits several features that are different from those of BR. The absorption maximum is blue-shifted, from 568 nm in

† This work was supported by National Institutes of Health Grant GM29498 and Department of Energy Grant DEFG03-86ER13525 (to J.K.L.).

* To whom correspondence should be addressed. Phone: (949) 824-7783. Fax: (949) 824-8540. E-mail: balashov@uci.edu.

‡ University of California.

§ Hokkaido University.

|| The Weizmann Institute of Science.

10.1021/bi050438h CCC: $30.25
Published on Web 07/19/2005

BR to 526−488 nm in different PR species (*21*, *22*). Light absorption initiates a photocycle which includes intermediates K, M, N, and O, in many aspects similar to those of BR (*24*−*26*) but with several significant differences: the L intermediate was not detected, the M intermediate decays faster than in bacteriorhodopsin, and the red-shifted intermediate at the end of its photocycle has a 13-cis retinal configuration rather than all-trans as in the O state of the BR photocycle (*24*). Many of the key residues involved in proton transport in bacteriorhodopsin are conserved in proteorhodopsin. This includes Asp97, the proton acceptor and Schiff base counterion (homologous to Asp85 in BR), Asp227 (Asp212 in BR), a residue close to the Schiff base and the C13═C14 bond of the chromophore and also part of the counterion, and others. The pK_a of proton acceptor Asp97 is much higher than that of Asp85 in BR (7.6 vs 2.6). This shift in pK_a correlates with a shift in the pK_a of proton pumping (*1*, *23*). The internal proton donor in BR, Asp96, is conservatively substituted with a residue with a longer side chain, Glu108, which efficiently reprotonates the Schiff base during the M to N transition in PR (*24*). The order of light-induced proton release and uptake during the photocycle is reversed in PR compared to that in bacteriorhodopsin (*24*). These and other differences suggest that studying PR and its mutants is likely to provide new insights into the mechanism of light-induced proton transport and its relationship to chromophore photoconversions.

One of the key residues in the chromophore binding site conserved among all archaeal retinal proteins and all proteorhodopsins is Asp227, homologous to Asp212 in BR. In previously reported work, we found evidence that as in BR, this aspartate has a very low pK_a (*27*). Illumination of proteorhodopsin at low pH results in the accumulation of a long-lived blue-shifted photoproduct absorbing at 430 nm (*27*). Its FTIR spectrum indicated that its chromophore is 9-*cis*. The yield of the 430 nm species in PR increases with a decrease in pH with a pK_a of 2.6, which is much lower than the pK_a of Asp97. The properties of the D227N mutant strongly suggested that this pK_a is for the protonation of Asp227: the pH dependence is largely eliminated, and the yield of the 430 nm species is enhanced in the mutant. These results indicate that the negative charge of Asp227 in the wild-type protein restricts formation of the long-lived photoproduct (*27*). This conclusion is consistent with earlier studies of the effects of neutralization of negatively charged residues on isomerization of the retinal in bacteriorhodopsin (*28*, *29*).

In the study presented here, we continue to explore the properties of PR. We describe long-lived photoproducts formed in the physiological pH range under conditions where the key group Asp97 is deprotonated. The D227N mutation facilitates accumulation of this long-lived photoproduct(s). At pH >9 for the wild-type protein and already above pH 7 for the D227N mutant, the photoconversions of the pigments appear to branch into a pathway leading to a formation of an M-like photoproduct absorbing at a shorter wavelength, 362 nm versus 400 nm in M, with the unusually long lifetime of 30 min and longer.

MATERIALS AND METHODS

The expression in *E. coli*, reconstitution with retinal, and purification of proteorhodopsin [the pseudo-wild-type triple-cysteine mutant, TCM, in which three cysteines are replaced with valines to prevent photooxidation (*1*)] and its D227N mutant were as described in our previous paper (*27*). Pigments solubilized in detergents (0.1% DM or 1% OG) were used.

Reconstitution of the proteorhodopsin with artificial retinal analogues was performed by addition of the analogues to cell membranes. We found that a substantially larger amount of the pigment was formed by reconstitution in the cell membranes rather than in the solubilized apoprotein. The membranes were obtained by breaking *E. coli* cells with a French press, and subsequent washing by several centrifugations as described previously (*24*). The retinal analogues dissolved in ethanol were added to the suspensions of the membranes in the presence of 100 mM NaCl and 20 mM phosphate buffer (pH 7.0). The final concentration of ethanol in the membrane suspension was below 1%. The formation of pigments was followed spectroscopically. Incorporation of all-trans retinal occurred with a time constant of ca. 15 min in both PR and the D227N mutant. Reconstitution of the all-trans retinal analogue locked in the C13═C14 bond was almost as rapid, but analogues locked in the C9═C10 bond and particularly in the C11═C12 bond incorporated slower, with time constants of ca. 1 and 4 h, respectively. In the latter case, the kinetics was biphasic and formation of an intermediate absorbing at 440−450 nm was observed. The photoconversions of the pigments were studied both in membranes (in the presence of 50% glycerol to reduce light scattering and prevent fast sedimentation of the membranes in the cuvette) and in a detergent solution. The two sets of experiments produced similar results.

The chromophore extraction from the initial (dark-adapted) pigment and that from the pigment after its illumination at wavelengths longer than 500 nm were performed under dim red light as described previously (*30*) with minor changes. Briefly, extraction of retinal oxime was carried out by hexane after denaturation by addition of a final concentration of 50% methanol and 90 mM hydroxylamine. To produce the 360 nm photoproduct, the samples were illuminated at 4 °C for 10 and 3 min for WT and D227N, respectively. The light source was a 1 kW slide projector filtered through a 520 nm cutoff filter (>500 nm) and a 1% $CuSO_4$ solution for removal of heat radiation. A high-performance liquid chromatograph was equipped with a silica column (6 mm × 150 mm, YMC-0123, Yamamura, Kyoto, Japan) with a detection wavelength of 360 nm. The solvent was composed of 12% (v/v) ethyl acetate and 0.12% (v/v) ethanol in hexane; the flow rate was 1.0 mL/min. The molar compositions of the retinal isomers were calculated form the areas of peaks in the HPLC elution using the following extinction coefficients (ϵ_{360}, in hexane): 54 900 M^{-1} cm^{-1} for all-trans 15-syn, 51 600 M^{-1} cm^{-1} for all-trans 15-anti, 49 000 M^{-1} cm^{-1} for 13-cis 15-syn, 52 100 M^{-1} cm^{-1} for 13-cis 15-anti, 35 000 M^{-1} cm^{-1} for 11-cis 15-syn, and 29 600 M^{-1} cm^{-1} for 11-cis 15-anti (*31*).

[1] Abbreviations: BR, bacteriorhodopsin; PR, proteorhodopsin; TCM, pseudo-wild-type triple-cysteine mutant of proteorhodopsin in which three cysteines are replaced with valines to prevent photooxidation (*1*) [in this paper, it is often called wild type (WT)]; OG, *n*-octyl β-D-glucopyranoside; DM, *n*-dodecyl β-D-maltopyranoside.

Absorption spectra were measured on a Shimadzu UV 1601 spectrophotometer at room temperature. Actinic light was from a Cole-Palmer 9741-50 illuminator equipped with 150 W halogen bulb and fiber optic light guide. The intensity of the 520 nm light (bandwidth of 10 nm) was ~2 mW/cm^2, and that of the >530 nm light was 15 mW/cm^2. The intensity of the 364 nm light (bandwidth of 70 nm) was ca. 1 mW/cm^2. Absorption measurements at low temperature were performed on a homemade cryostat.

The quantum efficiency for the formation of a long-lived photoproduct (P362) was estimated by measuring the light-induced absorption changes of wild-type proteorhodopsin and the D227N mutant at the absorption maximum (ΔA_{PR}) produced by illumination with 530 nm monochromatic light, and comparing them with absorption changes of dark-adapted bacteriorhodopsin under short-term illumination with the same light (ΔA_{LA}). The illumination time, t_{BR} and t_{PR}, was such that only small fraction of the pigment was converted in both cases (<10%). The quantum efficiency of light adaptation of bacteriorhodopsin (photoisomerization from 13-cis 15-syn to all-trans chromophore configuration) was taken to be ca. 0.06 ($\Phi_{LA} = 0.06$), an order of magnitude lower than the efficiency of the photocycle of trans BR (*32*) as estimated in refs *33*−*35*. Using the value given above for the quantum efficiency for dark adaptation of BR, the extinction coefficients for PR (ϵ_{PR}) and all-trans BR at the absorption maximum (43 900 and 63 000 M^{-1} cm^{-1}, respectively), and taking into account that absorption changes due to light adaptation at 585 nm are equal to 0.2 of the maximum absorbance of all-trans BR, and that the extinction coefficients of all-trans and 13-cis at 530 nm are equal, while the fractions of 13-cis in the dark-adapted state (f_c) equals 0.6, the quantum efficiency of conversion of proteorhodopsin to the P362 nm species (Φ_{P362}) could be calculated from the formula

$$\Phi_{P362} = 0.2\Phi_{LA}\Delta A_{PR}\epsilon_{BR}(1 - T_{BR})t_{BR}f_c/\Delta A_{LA}\epsilon_{PR}(1 - T_{PR})t_{PR} \approx 0.01\Delta A_{PR}(1 - T_{BR})t_{BR}/\Delta A_{LA}(1 - T_{PR})t_{PR}$$

where T_{BR} and T_{PR} are the transmissions of the samples at 530 nm.

RESULTS

Reversible Photoconversion of the WT and the D227N Mutant to a Long-Lived 362 nm Species. Both in the wild type and in the D227N mutant, illumination above neutral pH caused the formation of very long-lived M-like photoproducts absorbing at 362 nm. The photoproducts were produced by 532 nm laser flashes (Figure 1), and by continuous light (Figure 2). The 362 nm photoproduct is produced much more effectively in D227N, but can be also observed in the wild-type protein when the illumination is at high pH (Figure 3). Unlike in D227N, in the wild type the yield of the photoproduct is negligible at pH 8 but increases with an increase in pH (Figure 4). The quantum efficiency at pH 10 is ~0.02.

In the WT and D227N, the photoreaction that produces the 362 nm species occurs with apparent pK_a values of 9.6 and 7.5, respectively (Figure 4). These values are well below the pK_a for deprotonation of the Schiff base in the dark, which is 11.3 for the WT and 10.4 for D227N (*27*). In the following, we will examine the new photoreaction as it occurs in the D227N mutant. At pH 8.5, the D227N chromophore absorbs at 512 nm (in 0.1% DM). Upon illumination at 520 nm, most of the pigment undergoes transformation to the long-lived photoproduct (Figure 2A,B). The strongly blue shifted maximum of the photoproduct at 362 nm indicates that its formation involves deprotonation of the Schiff base. The ratio of the absorption changes at 362 and 512 nm is 0.5. This is 1.5-fold greater than the analogous ratio for the long-lived 430 nm photoproduct that is formed at low pH (*27*).

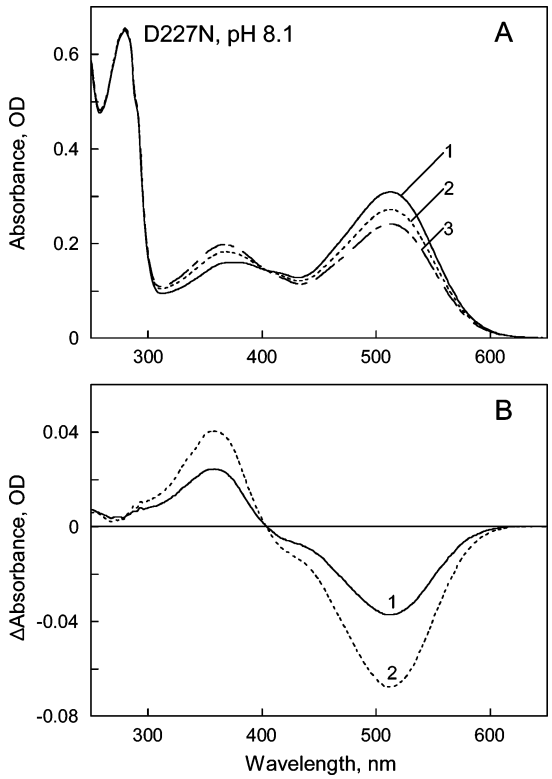

FIGURE 1: Conversion of the D227N pigment to a short wavelength photoproduct by 532 nm laser flashes. (A) Absorption spectra of (1) the initial pigment, (2) the pigment after 10 flashes, and (3) the pigment after 10 additional flashes. The flashes were given with 10 s intervals to allow relaxation of the photocycle intermediates from a preceding flash. The sample was not illuminated with continuous light capable of causing photoconversion of the pigment. (B) Curves 1 and 2 are difference spectra obtained by subtracting curve 1 in panel A from curves 2 and 3, respectively.

The quantum efficiency of the photoconversion to the 362 nm species at pH 8.5 is very high, ~0.2, in the D227N mutant. This value was obtained from a comparison of the yield of the 362 nm species with the rate of light adaptation of bacteriorhodopsin. Thus, the quantum yield of the 362 nm species at pH 8.5 is ~20-fold higher than for the 430 nm species at pH 4 in the same mutant (*27*).

Upon incubation in the dark, the 362 nm photoproduct slowly converts back to the initial state (Figure 2A,B) with a time constant of 30 min (Figure 2C). This is more than 3 orders of magnitude slower than the photoconversion of the M intermediate in the photocycle (*24*).

Illumination with 364 nm light converts a large fraction of the 362 nm photoproduct back to the initial pigment (Figure 5). Only a small fraction remains after prolonged illumination, because light at this wavelength drives both forward and reverse photoreactions and leads to a photo-

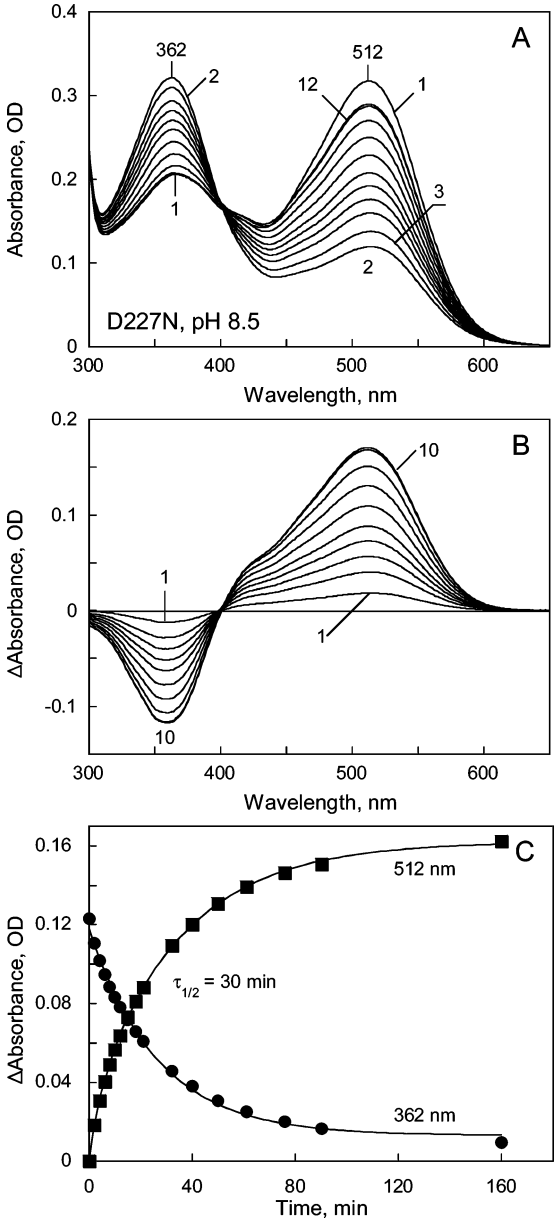

FIGURE 2: Light-induced conversion of the D227N mutant of proteorhodopsin to a 362 nm photoproduct and reverse thermal transition in the dark. (A) Absorption spectra of (1) the initial pigment at pH 8.5, (2) the pigment after illumination for 30 s at 520 nm, and (3−12) the pigment after incubation in the dark for 2, 6, 10, 15, 21, 32, 50, 90, 260, and 330 min after illumination, respectively. (B) Curves 1−10, obtained as the difference of "curve *i* minus curve 2", where curves *i* are curves 3−12 in panel A. (C) Kinetics of absorption changes at 512 and 362 nm.

steady state mixture. The 520 nm light converts nearly all the pigment into the 362 nm form. Thus, by alternating illuminations with 364 and 520 nm light, the pigment can be switched reversibly between two states (absorbing at longer wavelength and short wavelength forms).

Evidence that Asp97 Is Deprotonated in the 362 nm Species. The 362 nm absorption maximum is shorter than that of the M intermediate (ca. 400 nm; see below). A likely explanation for this is that Asp97 is deprotonated in the 362 nm photoproduct. Two lines of evidence support this.

The first is from low-temperature experiments. In BR and phoborhodopsin, illumination of the M intermediate trapped at low temperatures with blue light causes photoisomerization

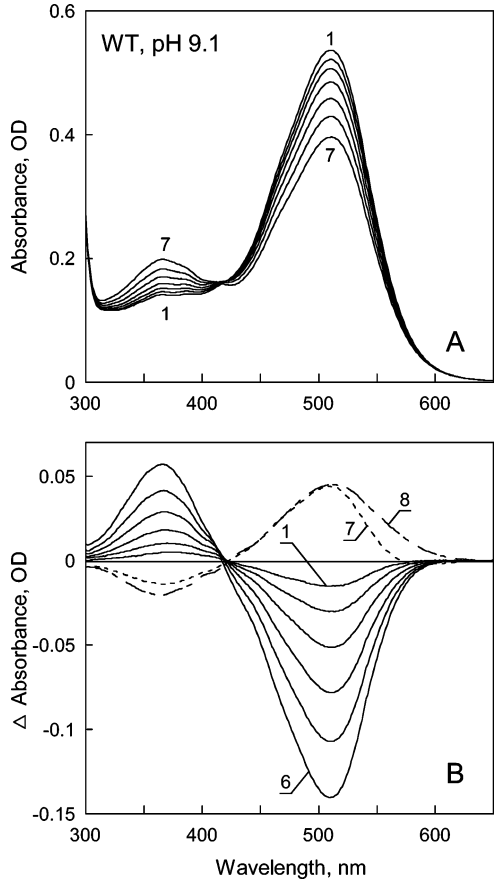

FIGURE 3: Light-induced formation of the 362 nm species in WT at pH 9.1. (A) Traces 1−7 are absorption spectra of the initial PR and the PR after illumination at >530 nm for 15, 45, 105, 225, 465, and 945 s, respectively. (B) Traces 1−6 are difference spectra obtained upon illumination at >530 nm, and trace 7 is the spectrum after 40 min in the dark after illumination at >530 nm and trace 8 after subsequent illumination at 364 nm.

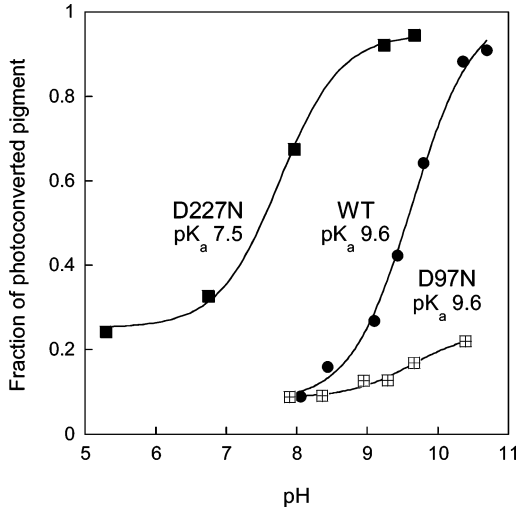

FIGURE 4: pH dependence of the fraction of the long-lived photoproducts in D227N and D97N mutants and WT PR produced by illumination for 1 min at >530 nm. The fraction was calculated from the light-induced decrease in the absorbance of the main band. The background level of photoconversion of the D227N mutant at pH below 7 is caused by its transformation to the 430 nm photoproduct as described previously (*27*).

of the chromophore, followed by fast reprotonation of the Schiff base by reverse proton transfer from Asp85. It occurs

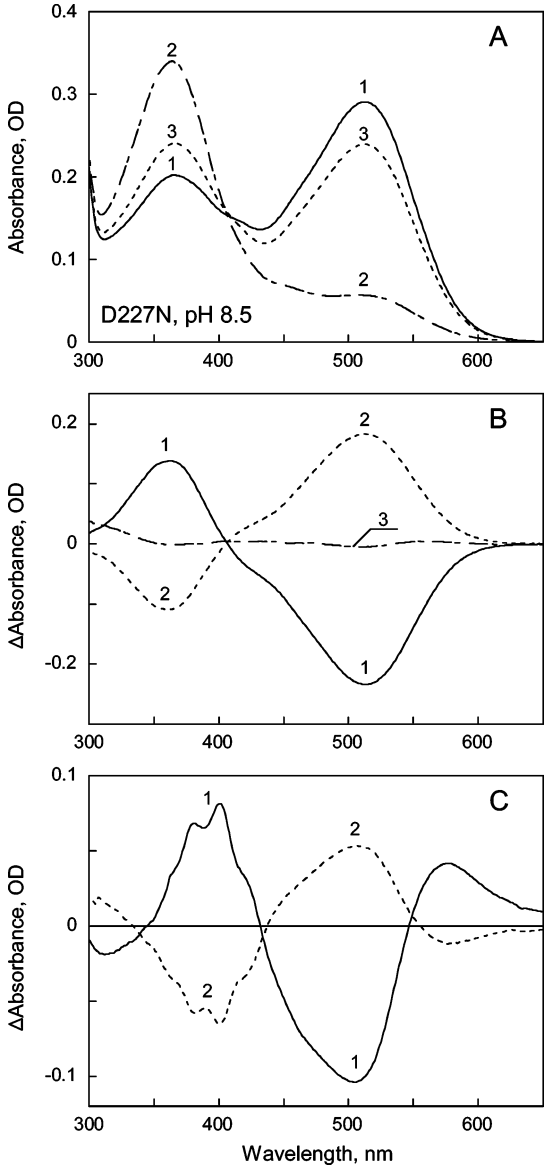

FIGURE 5: (A) Photoconversion of the D227N mutant to the 362 nm species at pH 8.5 and reverse photoconversion of the 362 nm species back to the initial pigment: absorption spectra at 295 K of (1) the initial D227N pigment, (2) the pigment after illumination for 3 min at 520 nm, and (3) the pigment after illumination for 2 min at 364 nm. (B) Difference spectra produced by (1) illumination at 520 nm (curve 2 minus curve 1 in panel A), (2) subsequent illumination with 364 nm light (curve 3 minus curve 2 in panel A), and (3) difference spectrum upon illumination of a sample containing 362 nm species (analogous to sample 2 in panel A but containing 66% glycerol) at 200 K with 364 nm light. The absence of absorption changes indicates no photoconversion of the 362 nm species takes place at 200 K. (C) Formation and photoconversion of the M intermediate of D227N at low temperatures. (1) Absorption changes accompanied formation of M (and some fraction of K) upon illumination of a water/glycerol (1:2) suspension of the D227N mutant in 0.1% DM and 100 mM NaCl for 5 min with 480−530 nm light during cooling from 230 to 200 K (the spectra before and after illumination were recorded at 200 K). (2) Absorption changes produced by a subsequent 5 min illumination at 407 nm.

even below 200 K (*36*−*39*). A similar photoreaction occurs also with the M intermediate of the D227N mutant at 200 K (Figure 5C). In contrast, illumination of the 362 nm species at 200 K does not cause reprotonation of the Schiff base (Figure 5B, curve 3). It occurs only at higher temperatures (>250 K). This would be explained if no proton were

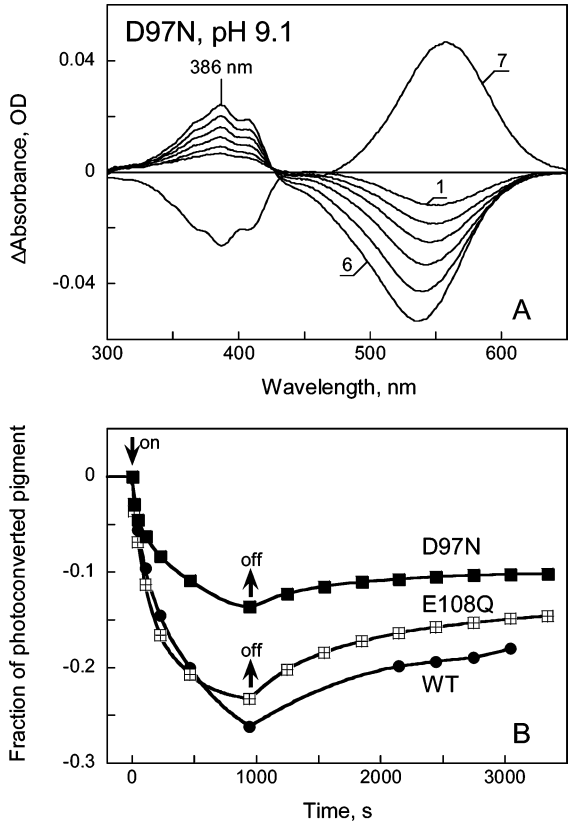

FIGURE 6: (A) Curves 1−6 are difference spectra obtained upon illumination of the D97N mutant at >530 nm for 15, 45, 105, 225, 465, and 945 s, respectively; trace 7 shows the light-induced absorption changes caused by illumination at 364 nm. The photoproduct of this reaction exhibits an absorption band at longer wavelengths than the initial state, but it relaxes thermally to the latter in the dark. (B) Fractions of light-induced conversion of wild-type PR, the D97N mutant, and the E108Q mutant to a long-lived photoproduct at pH 9.1. The pigments were solubilized in 0.1% DM and 100 mM NaCl.

available at Asp97 to reprotonate the Schiff base in the initial photoproduct of the 362 nm species. Another relevant observation is that the 362 nm species does not form below 230 K. Illumination of the D227N mutant during cooling from 230 to 200 K at 480−530 nm caused formation of the M intermediate and the red-shifted species, most likely K, but the 362 nm species did not accumulate (see curve 1 in Figure 5C). This indicates also that the formation of the 362 nm species does not precede M; it is highly temperature-dependent and appears after M is formed.

The second piece of evidence is from photoconversion of the D97N mutant, in which residue 97 cannot be anionic. Illumination of D97N mutant at high pH also results in formation of a long-lived photoproduct with deprotonated Schiff base, but with a red-shifted absorption maximum relative to those of the wild type and D227N, from 362 to 386 nm (Figure 6A). The latter is as expected, since neutralization of Asp97 causes a ca. 30 nm red shift of the absorption maximum of PR and its deprotonated form (*27*). The yield of the short wavelength photoproduct and quantum efficiency of its formation is lower than in the wild type (Figure 6 B) and manyfold lower than in D227N mutant, indicating that neutralization of the two aspartates near the chromophore has different effects on formation of the long-lived photoproducts. Neutralization of the proton donor E108Q, on the other hand, does not cause any substantial

change in the accumulation of the long-lived photoproduct compared to the wild type (Figure 6B).

Acceleration of the Decay of the 362 nm Photoproduct by Lowering the pH. If the difference between M produced in the normal photocycle and the 362 nm species is in the protonation state of some residue, perhaps Asp97 as discussed above, then one might expect that the pH would influence the decay of the 362 nm species. Alternatively, if the 362 nm species is the product of hydrolysis of the Schiff base, as was shown for the short wavelength 9-cis photoproduct of BR (*40*), decreasing the pH would not affect the absorption maximum in a strong way. These possible alternative explanations were tested in pH-jump experiments where the 362 nm species was produced at pH 8.2, and then the pH was rapidly decreased from 8.2 to 4. As shown in curve 3 of Figure 7A and curve 1 of Figure 7B, the 362 nm species (deprotonated Schiff base) rapidly and completely converts to a species absorbing around 440 nm (protonated Schiff base) and the initial 518 nm pigment after the pH shift. Subsequently, all or nearly all of the 440 nm species converts to the 518 nm pigment in a biphasic reaction with time constants of 30 s (60%) and 6 min (40%). This is faster than the thermal conversion of the 362 nm pigment at pH 8.5 (Figure 2C), although still much slower than the decay of M in the photocycle. These data suggest that recovery of the initial state is accelerated upon reprotonation of the Schiff base and Asp97 from the bulk, and imply therefore that the 362 nm species is not a product of hydrolysis of the Schiff base. The slower recovery compared to the M intermediate indicates that these states differ in the configuration of the chromophore or the conformation of the protein.

Reconstitution and Photoconversion of the D227N Mutant with Retinal Analogues that Restrict Isomerization around the C9═C10, C11═C12, and C13═C14 Bonds. Experiments with retinal analogues were undertaken to identify the double bond whose rotation is involved in the formation of the 362 nm species. The three analogues that were used (Figure 8A,B) which selectively block isomerization around the C9═C10, C11═C12, or C13═C14 bond, but allow isomerization around the other double bond(s). The C9═C10 locked analogue in D227N has a chromophore with an absorption maximum similar to one with native retinal (522 nm vs 523 nm at pH 6.9, respectively). The C11═C12 locked analogue resulted in a somewhat blue-shifted spectrum at 514 nm. In contrast, the C13═C14 locked analogue produced a considerably red-shifted chromophore with a maximum at 549 nm and a shoulder at 500 nm. In the wild type, the maximum is at 551 nm. The red shift indicates that the conformation of the retinal locked in the C13═C14 all-trans configuration is somewhat different from the native chromophore. This could be caused by different torsion angles of the C12−C13═C14 bonds in the native form and the locked analogue. If a twist in the C12−C13 bond in the native chromophore resulted in a blue shift of the maximum, introduction of a ring would lead to a more planar chromophore and a red shift.

Illumination at pH 8.1 converted the D227N pigments reconstituted with the C9═C10 and C11═C12 locked analogues to short-wavelength photoproducts absorbing at 347 and 358 nm, respectively (Figure 9A,B), with a quantum efficiency close to that of the native chromophore (Figure 8B). The blue-shifted maximum of the photoproduct of the C9═C10 locked pigment (347 vs 362 nm for native retinal)

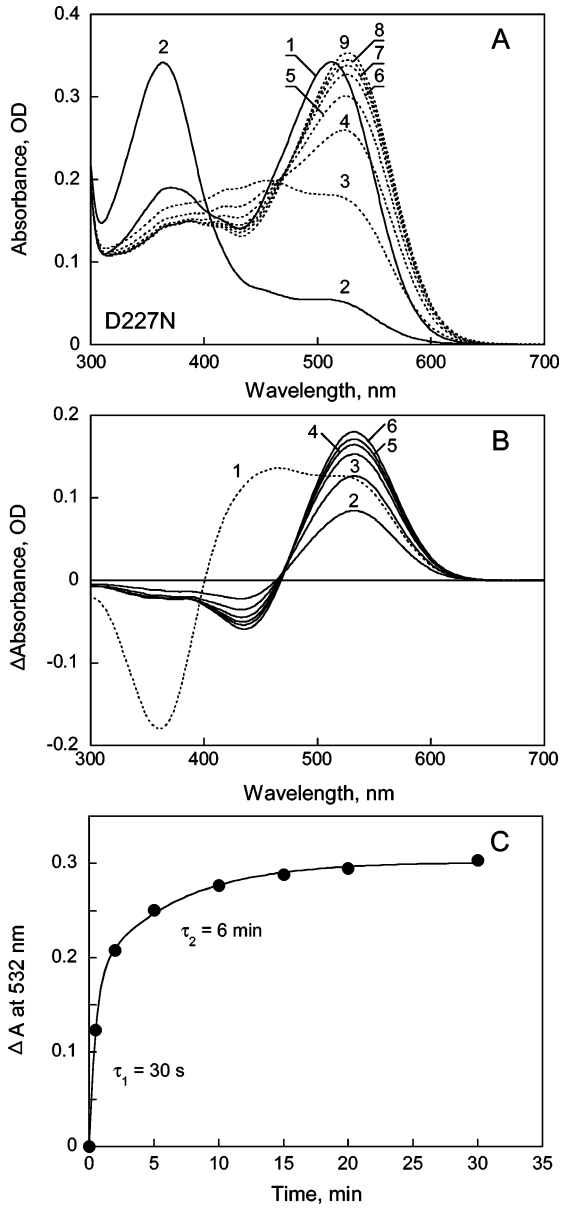

FIGURE 7: Acceleration of the decay of the 362 nm photoproduct of the D227N mutant with a shift in pH from 8.2 to 4. (A) Absorption spectra of (1) D227N at pH 8.2, (2) the pigment after illumination for 3 min at 520 nm, (3) the pigment after the subsequent shift of the pH to 4, and (4−9) the pigment in the dark for 2, 5, 10, 15, 20, and 30 min, respectively, after the shift in pH. (B) Difference spectra: (1) curve 3 minus 2 in panel A and (2−6) curves obtained by subtracting spectrum 3 in panel A from spectra 4−9. (C) Kinetics of recovery of the initial pigment at pH 4 and its fit with two components.

is as expected because the absorption maximum of the C9═C10 locked retinal analogue in solution, with unprotonated Schiff base, is also considerably blue-shifted (to 335 nm). As with the native chromophore, this photoconversion was thermally reversible on a time scale of tens of minutes. These data indicate that the formation of the long-lived photoproduct absorbing around 360 nm is not inhibited by blocking rotation around the C9═C10 or C11═C12 double bonds, and we conclude that the photoconversion to the 362 nm species with native chromophore does not necessarily involve isomerization around these bonds.

The D227N pigment reconstituted with the C13═C14 locked retinal exhibited a quite different pattern (Figure 9C).

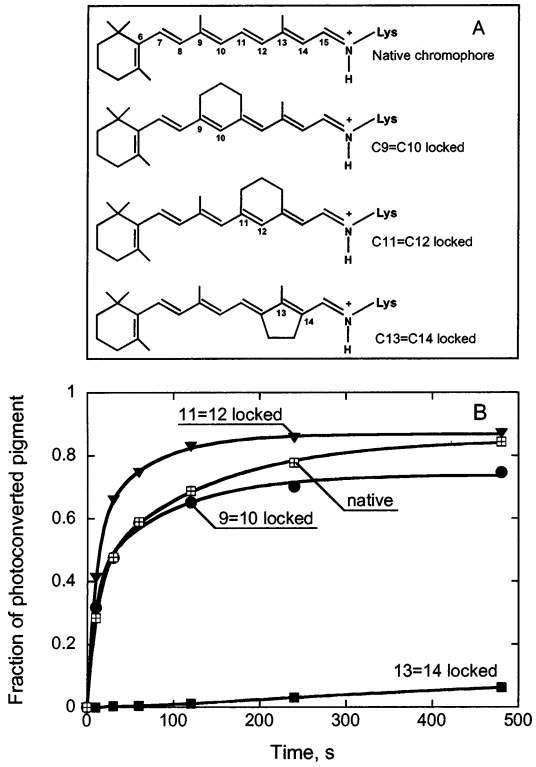

FIGURE 8: (A) Structures of the all-trans chromophore and artificial analogues used in this study. (B) Relative fraction of photoconversion of the D227N pigments reconstituted with all-trans retinal and its locked analogues upon illumination with 520 nm light. The pigments were solubilized in 1% OG. The difference spectra of light-induced conversions are given in Figure 9.

Illumination with 520 nm light for 1 min converted only a very small fraction of this pigment, far less than when isomerization is blocked in the C9═C10 bond, in the C11═C12 bond, or with the native chromophore. The difference spectrum obtained upon prolonged and more intense illumination at >530 nm light shows that the species that formed absorbs at 447 nm (Figure 9C). Unlike the 362 nm photoproduct observed in the C9═C10 locked pigment, the 447 nm photoproduct is thermally stable. This indicates that photoconversion of the C13═C14 locked analogue does not lead to the 360 nm species but yields a different photoproduct formed with much lower quantum efficiency (ca. 15-fold smaller than in the native pigment). The transformation into the 447 nm species was reversible with blue light. Prolonged illumination with 425 nm light caused re-formation of the 550 nm band of the initial pigment. It is reasonable to conclude that the limited photoreversible conversion into the 447 nm photoproduct involves isomerization around a double bond other than the C13═C14 bond. On the other hand, the absence of the 362 nm photoproduct in the C13═C14 locked analogue implies that its formation involves isomerization around this bond.

Extraction and HPLC Analysis of the Chromophore of the 362 nm Species. The long lifetime of the 362 nm photoproduct makes it possible to identify the isomeric state of its retinal by extraction and chromatographic analysis. The D227N mutant at pH 8.2 and the wild type at pH 10 were analyzed in this way before and after illumination with >520 nm light. Under these conditions, illumination converted 90% of the D227N mutant and 80% of the wild type. The retinal isomeric composition in the initial (dark-adapted) wild-type

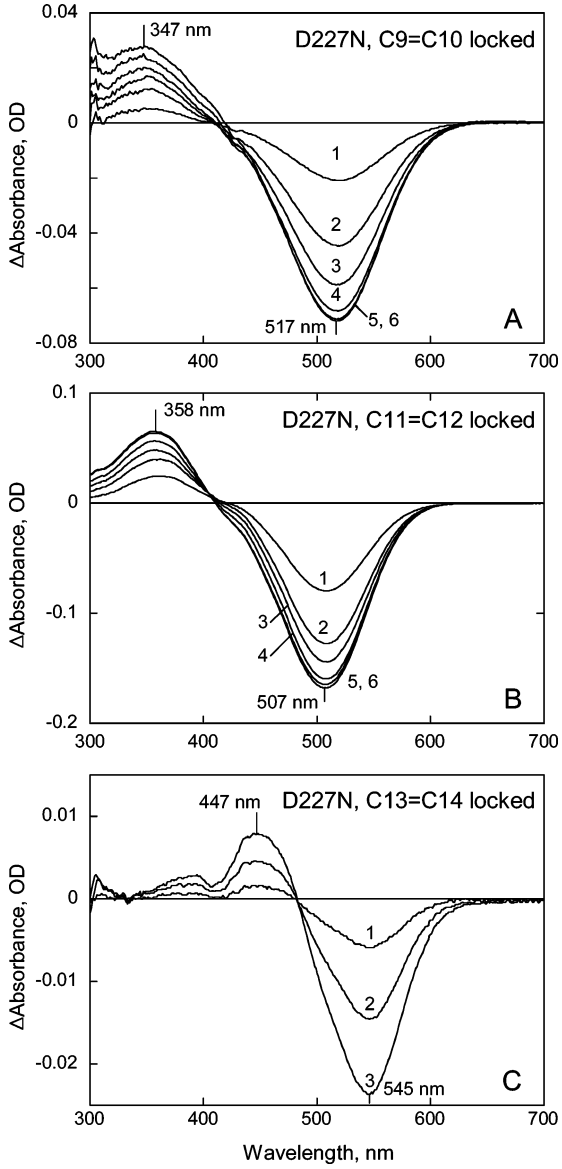

FIGURE 9: Light-induced absorption changes of the D227N pigment reconstituted with (A) the all-trans C9═C10 locked retinal analogue, (B) the all-trans C11═C12 locked retinal analogue, and (C) the all-trans C13═C14 locked analogue. In panels A and B, curves 1−6 were produced by illumination with 520 nm light for 10 s, 30 s, 1 min, 2 min, 4 min, and 8 min, respectively. In panel B, spectra 1−3 were produced by illumination for 1, 3, and 6 min, respectively, with a much more intense light at >530 nm.

Table 1: Retinal Isomeric Composition of Wild-Type Proteorhodopsin and the D227N Mutant before and after Illumination with >520 nm Light

	all-trans (%)	13-cis (%)	11-cis (%)
WT in the dark at pH 10.0	95.1	4.9	0.0
WT after illumination at pH 10.0	16.7	78.5	4.8
D227N in the dark at pH 8.4	74.7	3.5	21.8
D227N after illumination at pH 8.4	7.6	83.2	9.2

protein was almost entirely all-trans, with only a small fraction of 13-cis (5%). This agrees with recent FTIR data (*41*). After photoconversion of most of the pigment to the 360 nm species, the isomeric composition was found to be 80% 13-cis and 17% all-trans (Table 1). This result clearly shows that the 362 nm photoproduct is 13-cis. The analogous experiment with the D227N mutant produced a similar result,

but the initial dark-adapted state of D227N contained a substantial amount of 11-cis pigment as well (75% all-trans, 22% 11-cis, and 3% 13-cis). After illumination at >520 nm, the isomeric composition changed to 8% all-trans, 83% 13-cis, and 9% 11-cis. The results summarized in Table 1 indicate that in both the wild type and D227N the formation of the 362 nm species correlates well with conversion of all-trans retinal to 13-cis.

DISCUSSION

This study describes the formation of a long-lived photoproduct of proteorhodopsin with the unprotonated Schiff base at high pH, and examines its possible origin and dependence on residues close to the chromophore. We show that mutation of Asp227 to Asn greatly enhances the formation of this species. Our findings of these long-lived species absorbing around 360 nm (Figure 1), and the related forms with a protonated Schiff base absorbing at around 440 nm (Figure 7A), might provide an explanation for the presence of 13-cis species in the initial state (*25*) and observations of heterogeneity of proteorhodopsin as discussed in the FTIR study by Krebs et al. (*42*).

Interestingly, the D227N mutant exhibits several features different from those of the homologous D212N mutant of BR (*43*, *44*). The formation of the M photointermediate is accelerated in D227N at neutral pH; in the D212N BR mutant it is slowed, and its level of accumulation is greatly reduced or even absent at alkaline pH (*44*). Most prominently, the D227N mutant of PR exhibits a reversible transition to a long-lived photoproduct at pH 8, absorbing at 362 nm that contains a deprotonated Schiff base. It converts back to the initial pigment thermally in an extremely slow "photocycle", and can be reconverted by illumination also. No such photoproduct was described for the D212N mutant of BR. This implies that the chromophore environment is not quite the same in the two proteins. The possible causes of the unusually slow PR photocycle at high pH are discussed below.

Origin of the 362 nm Species. The short wavelength maximum of the 362 nm species implies that it has a deprotonated Schiff base. The chromophore extraction experiments and experiments with artificial analogues indicate that the 362 nm species is formed as a result of photoisomerization around the C13═C14 bond. The 362 nm species is formed not only under continuous light but also under short 6 ns 532 nm laser flashes given at time intervals long enough to allow for decay of the photocycle intermediates (Figure 1). This indicates that it is formed as a single quantum reaction originating from the initial state.

The 362 nm species has an absorption maximum at a shorter wavelength than the M intermediate of the photocycle. This would be explained if Asp97 in the 362 nm species were deprotonated, unlike in the M state where it is known to be protonated (*24*, *25*) (see Table 2). This idea is supported by the facts that in the D227N mutant the pK_a values of Asp97 and the Schiff base in the unphotolyzed state are lower than in the wild type (*27*) and the pK_a for the photoconversion efficiency to the 362 nm species is lower also (Figure 4). Furthermore, the different photoreactivities of the M intermediate and the 362 nm species at low temperatures (Figure 5B,C) can be explained by the absence of a proton on Asp97 in the 362 nm species, which prevents reprotonation of the Schiff base upon photoisomerization of the chromophore. Finally, the D97N mutant, in which Asp97 is neutralized, does not convert to the 362 nm species; instead, a photoproduct absorbing at 398 nm is formed (Figure 6).

Table 2: Configuration of the Chromophore and Protonation State[a] of Key Groups in PR, M, N, and P362

	configuration of the chromophore	Schiff base	Asp97	Glu108
PR	all-trans	+	−	+
M	13-cis	−	+	+
N	13-cis	+	+	−
P362	13-cis	−	−	?

[a] The plus sign stands for the protonated state and the minus sign for the deprotonated state.

Is the 362 nm species a photoproduct of a fraction of proteorhodopsin in which an acidic residue is unprotonated? If the pH dependence of the yield of this species (Figure 4) were to originate from photoconversion of the unprotonated form only, such a protonation equilibrium would have to be slower than the 10 min of illumination time. This seems very unlikely. It is more probable that the 362 nm species arises as a side reaction of the normal photocycle, and the pH dependence of the yield is from the pH-dependent competition of this branching with the reaction that leads to recovery of the initial state. At which step is this branch leading to the long-lived photoproduct? Deprotonation of which group is responsible for the titration-like increase in the yield of the photoproducts with pK_a values of 7.5 and 9.6 in D227N and wild-type PR? Our working hypothesis is that the branch is late in the photocycle, and the effect of the D227N residue replacement on it is through the decreased pK_a values of the Schiff base and Asp97 in the mutant. This is suggested by the observation that illumination at 210 K results in accumulation of the M intermediate but no 362 nm species are formed, strongly implying that the latter originates from branching of the pathway after the M intermediate is formed. In the E108Q mutant, M decay is so slow that little N accumulates (*1*). Because the 362 nm species is formed in the E108Q mutant approximately as well as in the wild type (Figure 6B), the branching point may well be at M. On the other hand, the high yield of the 362 nm photoproduct correlates with slowing of the reisomerization of the photocycle in the N state of the D227N mutant (not shown). It is likely that photoisomerization of the chromophore to 13-cis leads to a decrease in the pK_a of the Schiff base by at least 2.5 units. If the Schiff base is in equilibrium with the bulk, this would explain the appearance of the long-lived photoproduct with a deprotonated Schiff base at a pH as low as 7.5 in D227N and 9.6 in the wild type. Apparently, in the 362 nm species, the Schiff base equilibrates with the bulk, whereas in the M intermediate, both deprotonation of the Schiff base and its reprotonation are internal processes.

Thermal reconversion of the 362 nm species to the initial state includes, necessarily, reprotonation of the Schiff base, reisomerization of the chromophore, and recovery of the initial protein conformation. Reprotonation of the Schiff base strongly decreases the barrier for thermal reisomerization (*45*, *46*) and so does the protonation of the counterion, Asp85 in BR (*47*). Thus, transient protonation of the Schiff base and

its counterion in the 362 nm species should precede reisomerization of the chromophore from 13-cis to all-trans. In agreement with this, the recovery of the initial state is accelerated upon reprotonation of the Schiff base, as the pH-jump experiment from pH 8 to 4 indicates.

Thus, the enhanced formation of the 362 nm species in the D227N mutant can be partially explained by electrostatic perturbation of the Schiff base and its counterion caused by neutralization of Asp227, which result in a lower pK_a for the Schiff base and Asp97 in this mutant.

The presence of a considerable amount of 11-cis pigment in the initial state of the D227N mutant is in agreement with our earlier conclusion that neutralization of D227N strongly affects isomerization of the retinal (*27*). Small amounts of 11-cis and 9-cis isomers were found in the initial state of the D212N mutant of BR as well (*48*).

Why Does the 362 nm Photoproduct Have a Long Lifetime? Decreasing the pH strongly accelerates the thermal recovery of the 362 nm species, but the rate is still many orders of magnitude slower than for the M intermediate. This indicates that reprotonation of the Schiff base, and presumably Asp97, does not direct the 362 nm species to the pathway taken by the pigment in the "normal" photocycle. The rate-limiting factor for the recovery of the initial state might reside in the altered conformation of the chromophore and/or the protein. The nature of this constraint needs to be investigated further. A likely possibility is that isomerization around the C═N bond of the retinal might be involved, as during light−dark adaptation of BR and during formation of the Meta III intermediate in rhodopsin. In the absence of transducin, a significant fraction of this signaling state of rhodopsin with a deprotonated Schiff base undergoes a slow transition to a species with a protonated Schiff base, called Meta III, which is inactive as a signaling state and was suggested to serve for storage of the chromophore (*49*). Interestingly, the transition involves the thermal equilibrium of Meta II with Meta I and thermal isomerization of the C═N double bond of the chromophore (transition from the anti to the syn configuration) (*50*). The Meta II to Meta III transition can be induced also by UV light (*51*). According to recent data, Meta III converts partially to rhodopsin, Meta II, and isorhodopsin upon illumination (*50*). It is possible that C═N isomerization is involved in formation and thermal conversion of P362 also.

Is There a Physiological Role for the Transition of PR to the 362 nm Species? Currently, there is no evidence for such a role, but it is a possibility. The transformation to the long-lived 362 nm photoproduct is apparently a side reaction of the photocycle, caused by alteration of the normal reprotonation and reisomerization pathway of the Schiff base at high pH. One may speculate that this transition might be a response to high pH. The pH of seawater on the surface generally is 8.4 (*52*), so under most conditions, the P362 nm species should not accumulate in substantial amounts in wild-type PR. If the light intensity is high, however, up to 10% of the PR still might be transformed to the 362 nm species. Under these conditions, this photoproduct could serve as a signaling state for elevated pH and/or high-light intensity.

Proteorhodopsin and Its D227N Mutant as a Photochromic Material. The photochromic properties of retinal pigments have attracted attention and stimulated attempts to utilize them for photonic applications. In the case of BR, the photoreversibility of its photoconversions (*36*, *53*), the high photochemical and thermal stability of the protein, its dichroism, and nonlinear optical properties (*12*, *54*, *55*) were implemented in several devices and prototypes for optical information storage and image processing (*13*−*16*). In particular, the D96N mutant of BR, because of its long-lived deprotonated M state (*56*) from the absence of an internal proton donor, was utilized in a number of applications (*13*). Other mutants showed some promise for optical information storage, particularly the mutants of Asp85, a residue close to the chromophore's Schiff base and its proton acceptor as well as part of its counterion, i.e., D85N and especially D85N/V49A (*57*). These mutations affect the chromophore isomerization pathway so that along with the "normal" 13-cis photoproducts it leads to high yields of a long-lived 9-cis species, which were first found in wild-type BR at low pH (*58*) and in the deionized "blue membrane" (*59*, *60*). Some applications are based on the photochemical reactions involving the O intermediate [or the blue membrane which is present in small amounts even at high pH (*47*)] and its photoproduct called Q which is analogous to the pink membrane and its deprotonated form Q absorbing at 390 nm (*61*, *62*).

The photochemical features of proteorhodopsin and particularly the D227N mutant described in this study and our earlier study (*27*) make it interesting as a prospective photochromic material. These features include (a) the virtually complete light-induced transformation to a long-lived intermediate absorbing at 362 nm which is accompanied by a large spectral shift, (b) the very long lifetime of this photoproduct, which is substantially longer than that of the M intermediate of the D96N mutant of BR, the favorite material in a number of applications (*13*), and (c) the high quantum efficiencies of the formation and reversal of the 362 nm species. These features of the D227N proteorhodopsin pigment are suitable for applications dealing with dynamic (real time) information processing. In analogy with the transition of BR to the M intermediate, one should expect that the conversion of PR to 362 nm species should be accompanied by changes in the refractive index and thus might be used in a number of applications, such as holography, based on nonlinear properties of photochromic material and light-induced refractive index variations.

In conclusion, our study of the photoreactions of the D227N mutant shows that neutralization of Asp227 leads to accumulation of a very long-lived 362 nm photoproduct which is formed in the wild type also but at a higher pH. This species has a 13-cis chromophore. Potentially, it might serve as a signaling state for the high-pH conditions. It is photoactive, and under illumination with UV light converts to the initial state. This photochromic behavior might be utilized for sensing UV light and in artificial systems for optical recording and information processing.

REFERENCES

1. Dioumaev, A. K., Wang, J. M., Balint, Z., Váró, G., and Lanyi, J. K. (2003) Proton transport by proteorhodopsin requires that the retinal Schiff base counterion Asp-97 be anionic, *Biochemistry 42*, 6582−6587.
2. Oesterhelt, D. (1998) The structure and mechanism of the family of retinal proteins from halophilic archaea, *Curr. Opin. Cell Biol. 8*, 489−500.

3. Spudich, J. L., Yang, C. S., Jung, K. H., and Spudich, E. N. (2000) Retinylidene proteins: Structures and functions from archaea to humans, *Annu. Rev. Cell Dev. Biol. 16*, 365−392.
4. Lanyi, J. K., Ed. (2000) Special issue: Bacteriorhodopsin, *Biochim. Biophys. Acta 1460*, 1−239.
5. Balashov, S. P., and Ebrey, T. G. (2001) Trapping and spectroscopic identification of the photointermediates of bacteriorhodopsin at low temperatures, *Photochem. Photobiol. 73*, 453−462.
6. Lanyi, J. K. (1999) Bacteriorhodopsin, *Int. Rev. Cytol. 187*, 161−202.
7. Oesterhelt, D., and Stoeckenius, W. (1973) Functions of a new photoreceptor membrane, *Proc. Natl. Acad. Sci. U.S.A. 70*, 2853−2857.
8. Stoeckenius, W., Lozier, R. H., and Bogomolni, R. A. (1979) Bacteriorhodopsin and the purple membrane of *Halobacteria*, *Biochim. Biophys. Acta 505*, 215−278.
9. Ebrey, T. G. (1993) Light Energy Transduction in Bacteriorhodopsin, in *Thermodynamics of Membrane Receptors and Channels* (Jackson, M. B., Ed.) pp 353−387, CRC Press, Boca Raton, FL.
10. Lanyi, J. K. (2004) Bacteriorhodopsin, *Annu. Rev. Physiol. 66*, 665−688.
11. Kamo, N., Shimono, K., Iwamoto, M., and Sudo, Y. (2001) Photochemistry and photoinduced proton-transfer of *pharaonis* phoborhodopsin, *Biochemistry (Moscow) 66*, 1580−1587.
12. Vsevolodov, N. (1998) *Biomolecular Electronics. An Introduction via Photosensitive Proteins*, Birkhauser, Boston.
13. Hampp, N. (2000) Bacteriorhodopsin as a photochromic retinal protein for optical memories, *Chem. Rev. 100*, 1755−1776.
14. Oesterhelt, D., Bräuchle, C., and Hampp, N. (1991) Bacteriorhodopsin: A biological material for information processing, *Q. Rev. Biophys. 24*, 425−478.
15. Birge, R. R. (1990) Photophysics and molecular electronic applications of the rhodopsins, *Annu. Rev. Phys. Chem. 41*, 683−733.
16. Birge, R. R., Gillespie, N. B., Izaguirre, E. W., Kusnetzow, A., Lawrence, A. F., Singh, D., Song, Q. W., Schmidt, E., Stuart, J. A., Seetharaman, S., and Wise, K. J. (1999) Biomolecular electronics: Protein-based associative processors and volumetric memories, *J. Phys. Chem. B 103*, 10746−10766.
17. Béjà, O., Aravind, L., Koonin, E. V., Suzuki, M. T., Hadd, A., Nguyen, L. P., Jovanovich, S. B., Gates, C. M., Feldman, R. A., Spudich, J. L., Spudich, E. N., and DeLong, E. F. (2000) Bacterial rhodopsin: Evidence for a new type of phototrophy in the sea, *Science 289*, 1902−1906.
18. Béjà, O., Spudich, E. N., Spudich, J. L., Leclerc, M., and DeLong, E. F. (2001) Proteorhodopsin phototrophy in the ocean, *Nature 411*, 786−789.
19. Sabehi, G., Massana, R., Bielawski, J. P., Rosenberg, M., Delong, E. F., and Béjà, O. (2003) Novel Proteorhodopsin variants from the Mediterranean and Red Seas, *Environ. Microbiol. 5*, 842−849.
20. Venter, J. C., Remington, K., Heidelberg, J. F., Halpern, A. L., Rusch, D., Eisen, J. A., Wu, D., Paulsen, I., Nelson, K. E., Nelson, W., Fouts, D. E., Levy, S., Knap, A. H., Lomas, M. W., Nealson, K., White, O., Peterson, J., Hoffman, J., Parsons, R., Baden-Tillson, H., Pfannkoch, C., Rogers, Y.-H., and Smith, H. O. (2004) Environmental genome shotgun sequencing of the Sargasso Sea, *Science 304*, 66−74.
21. Man, D., Wang, W., Sabehi, G., Aravind, L., Post, A. F., Massana, R., Spudich, E. N., Spudich, J. L., and Béjà, O. (2003) Diversification and spectral tuning in marine proteorhodopsins, *EMBO J. 22*, 1725−1731.
22. Kelemen, B. R., Du, M., and Jensen, R. B. (2003) Proteorhodopsin in living color: Diversity of spectral properties within living bacterial cells, *Biochim. Biophys. Acta 1618*, 25−32.
23. Sineshchekov, O. A., and Spudich, J. L. (2004) Light-induced intramolecular charge movements in microbial rhodopsins in intact *E. coli* cells, *Photochem. Photobiol. Sci. 3*, 548−554.
24. Dioumaev, A. K., Brown, L. S., Shih, J., Spudich, E. N., Spudich, J. L., and Lanyi, J. K. (2002) Proton transfers in the photochemical reaction cycle of proteorhodopsin, *Biochemistry 41*, 5348−5358.
25. Friedrich, T., Geibel, S., Kalmbach, R., Chizhov, I., Ataka, K., Heberle, J., Engelhard, M., and Bamberg, E. (2002) Proteorhodopsin is a light-driven proton pump with variable vectoriality, *J. Mol. Biol. 321*, 821−838.
26. Váró, G., Brown, L. S., Lakatos, M., and Lanyi, J. K. (2003) Characterization of the photochemical reaction cycle of proteorhodopsin, *Biophys. J. 84*, 1202−1207.
27. Imasheva, E. S., Balashov, S. P., Wang, J. M., Dioumaev, A. K., and Lanyi, J. K. (2004) Selectivity of retinal photoisomerization in proteorhodopsin is controlled by aspartic acid 227, *Biochemistry 43*, 1648−1655.
28. Song, L., El-Sayed, M. A., and Lanyi, J. K. (1993) Protein catalysis of the retinal subpicosecond photoisomerization in the primary process of bacterial photosynthesis, *Science 261*, 891−894.
29. Logunov, S. L., El-Sayed, M. A., and Lanyi, J. K. (1996) Catalysis of the retinal subpicosecond photoisomerization process in acid purple bacteriorhodopsin and some bacteriorhodopsin mutants by chloride ions, *Biophys. J. 71*, 1545−1553.
30. Shimono, K., Ikeura, Y., Sudo, Y., Iwamoto, M., and Kamo, N. (2001) Environment around the chromophore in *pharaonis* phoborhodopsin: Mutation analysis of the retinal binding site, *Biochim. Biophys. Acta 1515*, 92−100.
31. Chen, P., Lee, T. D., and Fong, H. K. W. (2001) Interaction of 11-cis-retinol dehydrogenase with the chromophore of retinal G protein-coupled receptor opsin, *J. Biol. Chem. 276*, 21098−21104.
32. Govindjee, R., Balashov, S. P., and Ebrey, T. G. (1990) Quantum efficiency of the photochemical cycle of bacteriorhodopsin, *Biophys. J. 58*, 597−608.
33. Litvin, F. F., Balashov, S. P., and Sineshchekov, V. A. (1975) The investigation of the primary photochemical conversions of bacteriorhodopsin in purple membranes and cells of *Halobacterium* halobium by the low-temperature spectrophotometry method, *Bioorg. Khim. 1*, 1767−1777.
34. Kalisky, O., Goldschmidt, C. R., and Ottolenghi, M. (1977) Photocycle and light adaptation of dark-adapted bacteriorhodopsin, *Biophys. J. 19*, 185−189.
35. Korenstein, R., and Hess, B. (1977) Hydration effects on cis−trans isomerization of bacteriorhodopsin, *FEBS Lett. 82*, 7−11.
36. Litvin, F. F., and Balashov, S. P. (1977) New intermediates in the photochemical conversions of bacteriorhodopsin, *Biophysics 22*, 1157−1160.
37. Hurley, J. B., Becher, B., and Ebrey, T. G. (1978) More evidence that light isomerizes the chromophore of purple membrane protein, *Nature 272*, 87−88.
38. Maeda, A., Tomson, F. L., Gennis, R. B., Kandori, H., Ebrey, T. G., and Balashov, S. P. (2000) Relocation of internal bound water in bacteriorhodopsin during the photoreaction of M at low temperatures: An FTIR study, *Biochemistry 39*, 10154−10162.
39. Balashov, S. P., Sumi, M., and Kamo, N. (2000) The M intermediate of *Pharaonis* phoborhodopsin is photoactive, *Biophys. J. 78*, 3150−3159.
40. Fischer, U., Towner, P., and Oesterhelt, D. (1981) Light indiced isomerization, at acidic pH, initiates hydrolysis of bacteriorhodopsin to bacterio-opsin and 9-*cis*-retinal, *Photochem. Photobiol. 33*, 529−537.
41. Bergo, V., Amsden, J. J., Spudich, E. N., Spudich, J. L., and Rothschild, K. J. (2004) Structural changes in the photoactive site of proteorhodopsin during the primary photoreaction, *Biochemistry 43*, 9075−9083.
42. Krebs, R. A., Dunmire, D., Partha, R., and Braiman, M. S. (2003) Resonance Raman characterization of proteorhodopsin's chromophore environment, *J. Phys. Chem. B 107*, 7877−7883.
43. Otto, H., Marti, T., Holz, M., Mogi, T., Stern, L. J., Engel, F., Khorana, H. G., and Heyn, M. P. (1990) Substitution of amino acids Asp-85, Asp-212, and Arg-82 in bacteriorhodopsin affects the proton release phase of the pump and the p*K* of the Schiff base, *Proc. Natl. Acad. Sci. U.S.A. 87*, 1018−1022.
44. Needleman, R., Chang, M., Ni, B., Váró, G., Fornés, J., White, S. H., and Lanyi, J. K. (1991) Properties of Asp212-Asn bacteriorhodopsin suggest that Asp212 and Asp85 both participate in a counterion and proton acceptor complex near the Schiff base, *J. Biol. Chem. 266*, 11478−11484.
45. Tavan, P., Schulten, K., and Oesterhelt, D. (1985) The effect of protonation and electrical interactions on the stereochemistry of retinal Schiff bases, *Biophys. J. 47*, 415−430.
46. Tajkhorshid, E., Paizs, B., and Suhai, S. (1999) Role of isomerization barriers in the pK_a control of the retinal Schiff base: A density functional study, *J. Phys. Chem. B 103*, 4518−4527.
47. Balashov, S. P., Imasheva, E. S., Govindjee, R., and Ebrey, T. G. (1996) Titration of aspartate-85 in bacteriorhodopsin: What it says about chromophore isomerization and proton release, *Biophys. J. 70*, 473−481.
48. Song, L., Yang, D., El-Sayed, M., and Lanyi, J. K. (1995) Retinal isomer composition in some bacteriorhodopsin mutants under light and dark adaptation conditions, *J. Phys. Chem. 99*, 10052−10055.

49. Heck, M., Schadel, S. A., Maretzki, D., Bartl, F. J., Ritter, E., Palczewski, K., and Hofmann, K. P. (2003) Signaling states of rhodopsin. Formation of the storage form, metarhodopsin III, from active metarhodopsin II, *J. Biol. Chem. 278*, 3162−3169.
50. Vogel, R., Siebert, F., Mathias, G., Tavan, P., Fan, G. B., and Sheves, M. (2003) Deactivation of rhodopsin in the transition from the signaling state Meta II to Meta III involves a thermal isomerization of the retinal chromophore C═N double bond, *Biochemistry 42*, 9863−9874.
51. Ritter, E., Zimmermann, K., Heck, M., Hofmann, K. P., and Bartl, F. J. (2004) Transition of rhodopsin into the active Metarhodopsin II state opens a new light-induced pathway linked to Schiff base isomerization, *J. Biol. Chem. 279*, 48102−48111.
52. Dickson, A. G. (1993) The measurement of seawater pH, *Mar. Chem. 44*, 131−142.
53. Balashov, S. P. (1995) Photoreactions of the photointermediates of bacteriorhodopsin, *Isr. J. Chem. 35*, 415−428.
54. Burykin, N. M., Korchemskaya, E. Y., Soskin, M. S., Taranenko, V. B., Dukova, T. V., and Vsevolodov, N. N. (1985) Photoinduced anisotropy in Bio-Chrom films, *Opt. Commun. 54*, 68−70.
55. Borucki, B., Otto, H., and Heyn, M. P. (1998) Linear dichroism measurements on oriented purple membranes between parallel polarizers: Contribution of linear birefringence and applications to chromophore isomerization, *J. Phys. Chem. B 102*, 3821−3829.
56. Miller, A., and Oesterhelt, D. (1990) Kinetic optimization of bacteriorhodopsin by aspartic acid 96 as an internal proton donor, *Biochim. Biophys. Acta 1020*, 57−64.
57. Millerd, J. E., Rohrbacher, A., Brock, N. J., Chau, C. K., Smith, P., and Needleman, R. (1999) Improved sensitivity in blue-membrane bacteriorhodopsin films, *Opt. Lett. 24*, 1355−1357.
58. Maeda, A., Iwasa, T., and Yoshizawa, T. (1980) Formation of 9-*cis*- and 11-*cis*-retinal pigments from bacteriorhodopsin by irradiating purple membrane in acid, *Biochemistry 19*, 3825−3831.
59. Liu, S. Y., and Ebrey, T. G. (1987) The quantum efficiency for the interconversion of the blue and pink forms of purple membrane, *Photochem. Photobiol. 46*, 263−267.
60. Chang, C.-H., Liu, S. Y., Jonas, R., and Govindjee, R. (1987) The pink membrane: The stable photoproduct of deionized purple membrane, *Biophys. J. 52*, 617−623.
61. Popp, A., Wolperdinger, M., Hampp, N., Brauchle, C., and Oesterhelt, D. (1993) Photochemical conversion of the O-intermediate to 9-cis-retinal-containing products in bacteriorhodopsin films, *Biophys. J. 65*, 1449−1459.
62. Gillespie, N. B., Wise, K. J., Ren, L., Stuart, J. A., Marcy, D. L., Hillebrecht, J., Li, Q., Ramos, L., Jordan, K., Fyvie, S., and Birge, R. R. (2002) Characterization of the branched-photocycle intermediates P and Q of bacteriorhodopsin, *J. Phys. Chem. B 106*, 13352−13361.

BI050438H